

Deep Learning Assisted Calibrated Beam Training for Millimeter-Wave Communication Systems

Ke Ma, Dongxuan He, Hancun Sun, Zhaocheng Wang, *Fellow, IEEE*,
and Sheng Chen, *Fellow, IEEE*

Abstract

Huge overhead of beam training poses a significant challenge in millimeter-wave (mmWave) wireless communications. To address this issue, a wide beam based training method is proposed to calibrate the narrow beam direction according to the channel power leakage in this paper. To handle the complex nonlinear properties of the channel power leakage, deep learning is utilized to predict the optimal narrow beam directly. Specifically, three deep learning assisted calibrated beam training schemes are proposed. First, Convolution Neural Network (CNN) is adopted to implement the prediction based on the instantaneous received signals of wide beam training. Besides, we propose to perform the additional narrow beam training based on the predicted probabilities for further beam direction calibrations. In the second scheme, in order to enhance the robustness to noise, Long-Short Term Memory (LSTM) Network is adopted to track the movement of users and calibrate the beam direction according to the received signals of prior beam training. To further reduce the overhead of wide beam training, an adaptive beam training strategy is proposed, where partial wide beams are selected to be trained based on the prior received signals. Furthermore, two criteria, namely optimal neighboring criterion (ONC) and maximum probability criterion (MPC), are designed for the selection. To handle mobile scenarios, auxiliary LSTM is introduced to calibrate the directions of the selected wide beams more precisely. Simulation results demonstrate that our proposed schemes achieve significantly higher beamforming gain with smaller beam training overhead compared with the conventional counterparts.

Index Terms

Millimeter-wave communications, beam training, beam prediction, deep learning

I. INTRODUCTION

Benefit from the high transmission rates enabled by sufficient bandwidth resources, millimeter-wave (mmWave) communication has been one of the crucial technologies in the fifth-generation

(5G) wireless communication systems [1], [2]. However, mmWave signals suffer from more serious pathloss compared with the conventional Sub-6GHz communication systems [3]. Fortunately, the small wavelength of mmWave signals allows more antennas to be integrated into both base stations (BSs) and user equipments (UEs) [4]. Therefore, large antenna arrays can be equipped at BS and UE sides to implement directional beamforming, such that high pathloss could be compensated by the beamforming gain [5]–[7].

In order to enhance the received power of mmWave signals, beam training has been widely adopted to search the optimal transmitting and receiving beams with the maximum beamforming gain [8]–[12]. Since the beams are generally selected from the predefined codebook with limited size, the brute-force beam search is an efficient and straightforward beam training scheme, i.e., to exhaustively sweep all the transmitting and receiving beam pairs in the codebooks [8]. However, it could lead to overwhelmingly high training overhead. To address the problem, the two-level beam search scheme based on a hierarchical multi-resolution codebook was proposed in [9] and [10], where the first-level search aimed to find the optimal wide beam, then the second-level search confirmed the optimal narrow beam direction in the range of the selected wide beam. Another training overhead reducing scheme is the interactive beam search, where the candidate transmitting and receiving beams were swept separately [11], [12]. Nevertheless, the two-level and interactive beam search schemes still bring considerable training overhead. To further reduce the overhead of the two-level beam search, [13] proposed to calculate the optimal narrow beam based on the ratio of the beamforming gains between the selected wide beam and its neighboring wide beams, whereas this scheme is sensitive to noise and multipath interference.

Recently, deep learning has been broadly adopted to enhance the performance of wireless communications [14], [15]. In order to decrease the overhead of beam training, deep learning has been introduced to predict the optimal beam directly [16]–[22]. A coordinated beamforming scheme was proposed in [16], which used Convolutional Neural Network (CNN) to predict the optimal beam from the pilot signals received at multiple BSs. Besides, Deep Neural Network (DNN) was applied to determine mmWave beams based on the low-frequency channel state information (CSI) in [17] and [18]. Furthermore, [19] and [20] proposed to exploit cameras to assist the mmWave beam prediction based on deep learning tools. Nevertheless, the above studies in [16]–[20] rely on auxiliary information, which may not be available in most scenarios. Differently, [21] and [22] utilized DNN to predict the optimal beam according to the training results of the uniformly sampled beams. However, noise and multipath interference could degrade

its prediction accuracy seriously when the directions of the sampled beams are not adjacent to the dominant path.

Unfortunately, both conventional beam training schemes and deep learning based beam prediction schemes select the optimal beam according to the instantaneous channel information, where noise may lead to beam misalignment. Thanks to the stability of UE movements within a short time, prior channel information can be used to track UE locations and assist beam training [23]–[27]. The Extended Kalman Filter (EKF) has been widely applied to track the angle of the dominant path [23]–[25], whereas the method is hard to converge in practical scenarios due to multipath interference [26]. Differently, Long-Short Term Memory (LSTM) Network was adopted to infer the optimal mmWave beam at the target BS based on the prior CSI of the source mmWave BS [27]. However, the estimation of mmWave CSI may lead to huge overhead due to large antenna numbers.

Motivated by the feasibility of estimating the angle of the dominant path based on the channel power leakage in the received signals of mmWave beam training [22], [28], this paper proposes to calibrate the narrow beam direction by utilizing the received signals of wide beam training. Besides, the prior received signals are used to track the movement of UEs, which could further reduce beam misalignment caused by noise. Considering the complex nonlinear properties of the channel power leakage, we adopt deep learning to predict the optimal narrow beam directly.

In particular, three deep learning assisted calibrated beam training schemes are proposed. The first scheme leverages CNN to implement the prediction based on the instantaneous received signals of wide beam training. Since the prediction results are expressed as the probability that each candidate narrow beam is the optimal one, the additional narrow beam training according to the predicted probabilities can be performed to further calibrate beam directions. In the second scheme, in order to enhance the robustness to noise, LSTM is utilized to track the movement of UEs and calibrate the narrow beam direction according to the received signals of prior beam training. To further reduce the overhead of wide beam training, an adaptive beam training strategy is proposed in the third scheme, where partial wide beams are selected to be trained based on the received signals of prior beam training. Specifically, two criteria of the wide beam selection, namely optimal neighboring criterion (ONC) and maximum probability criterion (MPC), are designed, where ONC selects the neighboring wide beams of the previous predicted optimal narrow beam, while MPC selects the wide beams with the top predicted probabilities in the previous beam prediction. Moreover, since the optimal beam direction may

switch in mobile scenarios, auxiliary LSTM is introduced to predict the optimal wide beam corresponding to the current instant in advance for calibrating the directions of the selected wide beams more precisely. Simulation results demonstrate that our proposed schemes achieve significantly higher beamforming gain with smaller beam training overhead compared with the conventional counterparts.

The main contributions can be summarized as follows:

- We propose a wide beam based training method to predict the optimal narrow beam, where CNN is applied to implement the prediction.
- We propose to enhance the prediction accuracy by using the received signals of prior beam training, where LSTM is applied to extract the UE movement information for further calibrating the predicted beam direction.
- We propose an adaptive beam training strategy, where two criteria, namely ONC and MPC, are proposed to select partial wide beams to be trained based on the received signals of prior beam training. Moreover, we propose auxiliary LSTM to calibrate the directions of the selected wide beams more precisely.

The paper is organized as follows. In Section II, the channel model and beam training models are illustrated. Next, three proposed calibrated beam training schemes are introduced in Section III, IV and V, respectively. Section VI demonstrates the simulation results. Finally, the conclusions are provided in Section VII.

Notation: \mathbb{Z} is the set of integers, \mathbb{N}^* is the set of positive integers, and $\mathbb{C}^{m \times n}$ is the space of $m \times n$ complex matrices. \mathbf{A} is a matrix, \mathbf{a} is a vector, and \mathcal{A} is a set. \wedge denotes the logical AND operation. $R(\cdot)$ and $I(\cdot)$ denote the real and imaginary parts of complex variables. The transpose and conjugate transpose operators are denoted by $(\cdot)^T$, $(\cdot)^H$, respectively. $|\cdot|$ denotes the magnitude for complex numbers. $\|\cdot\|_2$ and $\|\cdot\|_\infty$ denote the 2-norm and infinite norm, respectively. \mathbf{I}_n is the $n \times n$ identity matrix. $\langle \cdot \rangle$ denotes the order statistics, i.e., assuming $\mathcal{A} = \{a_1, a_2, \dots, a_n\}$, $\langle \mathcal{A} \rangle = \{a_{\sigma_1}, a_{\sigma_2}, \dots, a_{\sigma_n}\}$, $a_{\sigma_1} \leq a_{\sigma_2} \leq \dots \leq a_{\sigma_n}$.

II. SYSTEM MODEL

A. Channel Model

The downlink mmWave multiple-input multiple-output (MIMO) communication system serving single user is considered, where BS and UE are equipped with M_{TX} and M_{RX} antennas, respectively. Besides, it is assumed that a single radio frequency (RF) chain is adopted at both

BS and UE sides. Since the line-of-sight (LOS) path with low attenuation can efficiently enhance the coverage of mmWave signals [29], [30], we consider the LOS scenario. For simplicity, we assume the two-dimensional (2D) channel model, where only azimuth angles are considered.

The narrowband geometric channel model consisting of one LOS path and C clusters is established [31]. Specifically, the channel matrix $\mathbf{H} \in \mathbb{C}^{M_{\text{RX}} \times M_{\text{TX}}}$ can be written as

$$\mathbf{H} = \underbrace{\sqrt{\frac{M_{\text{TX}} M_{\text{RX}}}{\rho_{\text{LOS}}}} \alpha_{\text{LOS}} \mathbf{a}_{\text{RX}}(\theta_{\text{LOS}}) \mathbf{a}_{\text{TX}}^H(\phi_{\text{LOS}}) +}_{\mathbf{H}_{\text{LOS}}} + \underbrace{\sum_{c=1}^C \sqrt{\frac{M_{\text{TX}} M_{\text{RX}}}{\rho_c}} \sum_{l=1}^{L_c} \frac{\alpha_{c,l}}{\sqrt{L_c}} \mathbf{a}_{\text{RX}}(\theta_c + \theta_{c,l}) \mathbf{a}_{\text{TX}}^H(\phi_c + \phi_{c,l})}_{\mathbf{H}_{\text{NLOS}}}, \quad (1)$$

where the c -th cluster containing L_c paths has pathloss ρ_c , angle-of-arrival (AoA) θ_c and angle-of-departure (AoD) ϕ_c , while $\alpha_{c,l}$, $\theta_{c,l}$, $\phi_{c,l}$ denote the complex gain, AoA offset, AoD offset corresponding to the l -th path in the c -th cluster. Besides, the variables with subscript LOS define corresponding parameters for the LOS path. For convenience, we use \mathbf{H}_{LOS} and \mathbf{H}_{NLOS} to represent the LOS part and the non line-of-sight (NLOS) part in the channel matrix, respectively. Furthermore, $\mathbf{a}_{\text{TX}} \in \mathbb{C}^{M_{\text{TX}} \times 1}$ and $\mathbf{a}_{\text{RX}} \in \mathbb{C}^{M_{\text{RX}} \times 1}$ denote the antenna response vectors of BS and UE. We assume that uniform linear arrays (ULAs) are adopted at both BS and UE sides, thus the antenna response vectors are expressed as

$$\mathbf{a}_{\text{TX}}(\phi) = \sqrt{\frac{1}{M_{\text{TX}}}} [1, e^{j2\pi d_{\text{TX}} \sin \phi / \lambda}, \dots, e^{j2\pi(M_{\text{TX}}-1)d_{\text{TX}} \sin \phi / \lambda}]^T, \quad (2)$$

$$\mathbf{a}_{\text{RX}}(\theta) = \sqrt{\frac{1}{M_{\text{RX}}}} [1, e^{j2\pi d_{\text{RX}} \sin \theta / \lambda}, \dots, e^{j2\pi(M_{\text{RX}}-1)d_{\text{RX}} \sin \theta / \lambda}]^T, \quad (3)$$

where d_{TX} and d_{RX} are the antenna spacings of BS and UE, λ denotes the wavelength, ϕ and θ denote the corresponding AoD and AoA. For simplicity, we set $d_{\text{TX}} = d_{\text{RX}} = \lambda/2$.

B. Beam Training Model

We assume that phase shifter based analog beamforming is applied, where $\mathbf{f} \in \mathbb{C}^{M_{\text{TX}} \times 1}$ aligned with the direction γ_{TX} is denoted as the transmitting beam of BS, and $\mathbf{w} \in \mathbb{C}^{M_{\text{RX}} \times 1}$ aligned with the direction γ_{RX} is denoted as the receiving beam of UE. The transmitting and receiving beams are selected from the predefined codebooks \mathcal{F} and \mathcal{W} , which consist of N_{TX} and N_{RX} candidate beams, respectively. Assuming the discrete Fourier transform (DFT) codebook is utilized [32], the

candidate transmitting beam $\mathbf{f}_m, m \in \{1, 2, \dots, N_{\text{TX}}\}$ and receiving beam $\mathbf{w}_n, n \in \{1, 2, \dots, N_{\text{RX}}\}$ can be written as

$$\mathbf{f}_m = \sqrt{\frac{1}{M_{\text{TX}}}} [1, e^{j\pi \sin \gamma_{\text{TX},m}}, \dots, e^{j\pi (M_{\text{TX}}-1) \sin \gamma_{\text{TX},m}}]^T, \quad (4)$$

$$\mathbf{w}_n = \sqrt{\frac{1}{M_{\text{RX}}}} [1, e^{j\pi \sin \gamma_{\text{RX},n}}, \dots, e^{j\pi (M_{\text{RX}}-1) \sin \gamma_{\text{RX},n}}]^T, \quad (5)$$

where $\gamma_{\text{TX},m}$ and $\gamma_{\text{RX},n}$ denote the beam directions of the m -th candidate beam at BS side and the n -th candidate beam at UE side, respectively. To cover the whole angular spaces of BS Γ_{TX} and UE Γ_{RX} , we assume that the transmitting and receiving beam directions are uniformly sampled in $(-\Gamma_{\text{TX}}/2, \Gamma_{\text{TX}}/2)$ and $(-\Gamma_{\text{RX}}/2, \Gamma_{\text{RX}}/2)$ [13], i.e.

$$\gamma_{\text{TX},m} = -\frac{\Gamma_{\text{TX}}}{2} + \frac{2m-1}{2N_{\text{TX}}} \Gamma_{\text{TX}}, \quad (6)$$

$$\gamma_{\text{RX},n} = -\frac{\Gamma_{\text{RX}}}{2} + \frac{2n-1}{2N_{\text{RX}}} \Gamma_{\text{RX}}. \quad (7)$$

Given the channel matrix \mathbf{H} and the applied beam pair $\{\mathbf{f}, \mathbf{w}\}$, the received signal y can be expressed as

$$y = \sqrt{P} \mathbf{w}^H \mathbf{H} \mathbf{f} x + \mathbf{w}^H \mathbf{n}, \quad (8)$$

where P is the transmit power and x is the transmitted signal satisfying $|x| = 1$. Besides, $\mathbf{n} \in \mathbb{C}^{M_{\text{RX}} \times 1}$ denotes additional white Gaussian noise (AWGN) $\mathbf{n} \sim \mathcal{CN}(0, \sigma^2 \mathbf{I}_{M_{\text{RX}}})$, where σ^2 is the noise power. Beam training targets to find the optimal beam pair $\{\mathbf{f}_{m_0}, \mathbf{w}_{n_0}\}$ with the maximum beamforming gain, which can be formulated as

$$\{m_0, n_0\} = \arg \max_{\substack{m \in \{1, 2, \dots, N_{\text{TX}}\}, \\ n \in \{1, 2, \dots, N_{\text{RX}}\}}} |\mathbf{w}_n^H \mathbf{H} \mathbf{f}_m|^2. \quad (9)$$

A straightforward scheme of beam training is the brute-force beam search, where all candidate transmitting and receiving beams are swept to find the beam pair with the maximum power of the received signal [8]. However, the scheme requires $N_{\text{TX}}N_{\text{RX}}$ measurements, which leads to overwhelmingly huge training overhead.

To tackle the problem, the two-level beam search based on a hierarchical multi-resolution codebook is considered, where the codebook consists of the wide beam codewords in the first level and the narrow beam codewords corresponding to Eq. (4) and (5) in the second level [9], [10]. For simplicity, we assume that the wide beams are obtained by switching on partial antennas [33], i.e., $M_{\text{TX}}/s_{\text{TX}}$ antennas are utilized to generate $N_{\text{TX}}/s_{\text{TX}}$ wide beams at BS side, where

$s_{\text{TX}} \in \mathbb{N}^*$ is defined as the number of narrow beams within each wide beam. Similarly, the wide beams at UE side can be implemented with $M_{\text{RX}}/s_{\text{RX}}$ antennas, where $s_{\text{RX}} \in \mathbb{N}^*$ denotes the number of narrow beams within each wide beam for UE. Therefore, the candidate transmitting wide beam $\mathbf{f}_{w,m}$, $m \in \{1, 2, \dots, N_{\text{TX}}/s_{\text{TX}}\}$ and receiving wide beam $\mathbf{w}_{w,n}$, $n \in \{1, 2, \dots, N_{\text{RX}}/s_{\text{RX}}\}$ can be written as

$$\mathbf{f}_{w,m} = \sqrt{\frac{1}{M_{\text{TX}}/s_{\text{TX}}}} [1, e^{j\pi \sin \gamma_{\text{TX},m}^w}, \dots, e^{j\pi(\frac{M_{\text{TX}}}{s_{\text{TX}}}-1) \sin \gamma_{\text{TX},m}^w}]^T, \quad (10)$$

$$\mathbf{w}_{w,n} = \sqrt{\frac{1}{M_{\text{RX}}/s_{\text{RX}}}} [1, e^{j\pi \sin \gamma_{\text{RX},n}^w}, \dots, e^{j\pi(\frac{M_{\text{RX}}}{s_{\text{RX}}}-1) \sin \gamma_{\text{RX},n}^w}]^T, \quad (11)$$

where the beam directions of the m -th candidate wide beam at BS side $\gamma_{\text{TX},m}^w$ and the n -th candidate wide beam at UE side $\gamma_{\text{RX},n}^w$ can be expressed as

$$\gamma_{\text{TX},m}^w = -\frac{\Gamma_{\text{TX}}}{2} + \frac{2m-1}{2N_{\text{TX}}} s_{\text{TX}} \Gamma_{\text{TX}}, \quad (12)$$

$$\gamma_{\text{RX},n}^w = -\frac{\Gamma_{\text{RX}}}{2} + \frac{2n-1}{2N_{\text{RX}}} s_{\text{RX}} \Gamma_{\text{RX}}. \quad (13)$$

Based on the hierarchical multi-resolution codebook, the beam search can be divided into two levels. The first-level search aims for coarse beam alignment based on the wide beam codebook, given by

$$\{m_0^w, n_0^w\} = \arg \max_{\substack{m \in \{1, 2, \dots, N_{\text{TX}}/s_{\text{TX}}\}, \\ n \in \{1, 2, \dots, N_{\text{RX}}/s_{\text{RX}}\}}} |\mathbf{w}_{w,n}^H \mathbf{H} \mathbf{f}_{w,m}|^2. \quad (14)$$

Next, the second-level search confirms the optimal narrow beam pair in the range of the selected wide beam pair, given by

$$\{m_0, n_0\} = \arg \max_{\substack{m \in \{(m_0^w-1)s_{\text{TX}}+1, \dots, m_0^w s_{\text{TX}}\}, \\ n \in \{(n_0^w-1)s_{\text{RX}}+1, \dots, n_0^w s_{\text{RX}}\}}} |\mathbf{w}_n^H \mathbf{H} \mathbf{f}_m|^2. \quad (15)$$

The two-level beam search requires $N_{\text{TX}}N_{\text{RX}}/s_{\text{TX}}s_{\text{RX}} + s_{\text{TX}}s_{\text{RX}}$ measurements, which could reduce the training overhead efficiently.

Another overhead reducing scheme is the interactive beam search, where the optimal beams at BS and UE sides are selected separately [11], [12]. Specifically, BS sweeps all candidate transmitting beams to find the beam with the maximum beamforming gain where UE antennas apply the omni-directional pattern, then UE sweeps all candidate receiving beams to find the beam with the maximum beamforming gain under the optimal transmitting beam. The optimal

beam pair can be obtained by combining two optimal beams at both BS and UE sides, which can be written as

$$m_0 = \arg \max_{m \in \{1, 2, \dots, N_{\text{TX}}\}} \|\mathbf{H}\mathbf{f}_m\|_2^2, \quad (16)$$

$$n_0 = \arg \max_{n \in \{1, 2, \dots, N_{\text{RX}}\}} |\mathbf{w}_n^H \mathbf{H}\mathbf{f}_{m_0}|^2. \quad (17)$$

The interactive beam search requires $N_{\text{TX}} + N_{\text{RX}}$ measurements, which could also decrease the training overhead significantly.

III. CNN ASSISTED CALIBRATED BEAM TRAINING

A. Motivation

As indicated in Eq. (16) and (17), the beam search can be implemented at BS and UE separately. For simplicity, here we investigate the selection of the transmitting beams at BS side, where the single-antenna UE is assumed thus the receiving beam \mathbf{w} is omitted.

Since mmWaves have weak penetration ability and significant reflecting power loss, the power of the LOS path is considerably higher than its NLOS counterparts, which indicates that the LOS path plays the dominant role in mmWave channels [34], [35]. To achieve the maximum beamforming gain, the transmitting beam direction γ_{TX} should be aligned with the AoD of the LOS path ϕ_{LOS} , while other NLOS paths can be treated as the noise. Specifically, we divide the channel matrix \mathbf{H} into its LOS part \mathbf{H}_{LOS} and NLOS part \mathbf{H}_{NLOS} , and rewrite the received signal model in Eq. (8) as

$$\begin{aligned} y &= \sqrt{P} \mathbf{H}_{\text{LOS}} \mathbf{f} x + \sqrt{P} \mathbf{H}_{\text{NLOS}} \mathbf{f} x + \mathbf{n} \\ &= \sqrt{P} \mathbf{H}_{\text{LOS}} \mathbf{f} x + \mathbf{n}_{\text{eq}}, \end{aligned} \quad (18)$$

where \mathbf{n}_{eq} denotes the equivalent noise including AWGN and NLOS paths. Substituting Eq. (1) into (18), the received signal can be further expressed as

$$y = \sqrt{\frac{M_{\text{TX}} M_{\text{RX}} P}{\rho_{\text{LOS}}}} \alpha_{\text{LOS}} \mathbf{a}_{\text{TX}}^H(\phi_{\text{LOS}}) \mathbf{f} x + \mathbf{n}_{\text{eq}}, \quad (19)$$

where $q(\phi_{\text{LOS}}) = \mathbf{a}_{\text{TX}}^H(\phi_{\text{LOS}}) \mathbf{f}$ reflects the alignment degree between γ_{TX} and ϕ_{LOS} , which determines the beamforming gain.

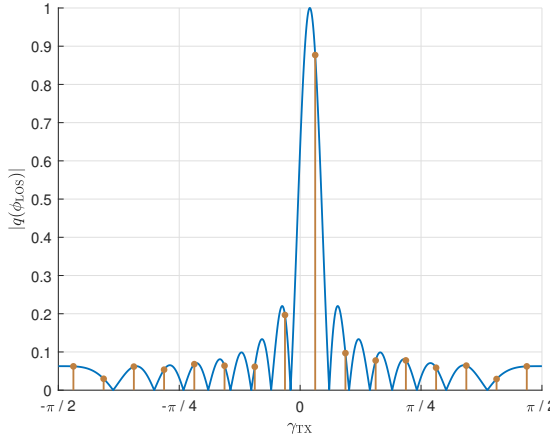


Fig. 1. An example of the channel power leakage, where the AoD of the LOS path $\phi_{\text{LOS}} = 0.02\pi$ and BS antenna number $M_{\text{TX}} = 16$. The blue line assumes that the transmitting beam direction γ_{TX} is continuously distributed in $[-\pi/2, \pi/2]$, while the brown dots show the results with $N_{\text{TX}} = 16$ candidate transmitting beams.

Due to the finite antenna number at BS side, the channel power leakage occurs in the received signals of beam training [28]. Specifically, assuming the m -th candidate transmitting beam is applied, we define $\mathbf{a}_{\text{TX}}^H(\phi_{\text{LOS}})\mathbf{f}_m$ as $q_m(\phi_{\text{LOS}})$, which can be calculated as

$$q_m(\phi_{\text{LOS}}) = \frac{1}{M_{\text{TX}}} \frac{\sin \frac{\pi M_{\text{TX}} \phi_m^\Delta}{2}}{\sin \frac{\pi \phi_m^\Delta}{2}} e^{j \frac{\pi (M_{\text{TX}}-1) \phi_m^\Delta}{2}}, \quad (20)$$

where $\phi_m^\Delta = \sin \gamma_{\text{TX},m} - \sin \phi_{\text{LOS}}$. If ϕ_{LOS} locates in the side lobe of the m -th candidate beam, i.e., $|\phi_m^\Delta| > 2/M_{\text{TX}} \wedge \phi_m^\Delta \neq 2k/M_{\text{TX}}, k \in \mathbb{Z}$, we have $|q_m(\phi_{\text{LOS}})| > 0$, which demonstrates that the power of the LOS path leaks to the m -th candidate beam. One example of the channel power leakage is illustrated in Fig. 1, where we can see that the relative relations of the elements in $\mathbf{q}(\phi_{\text{LOS}}) = [q_1(\phi_{\text{LOS}}), q_2(\phi_{\text{LOS}}), \dots, q_{N_{\text{TX}}}(\phi_{\text{LOS}})]$ are decided by ϕ_{LOS} . Further assuming the transmitted signal x is fixed and the equivalent noise \mathbf{n}_{eq} is omitted, the relative relations in $\mathbf{q}(\phi_{\text{LOS}})$ are reflected in the received signals, which provides the feasibility to estimate ϕ_{LOS} based on the received signals of beam training.

B. Problem Formulation

In order to reduce the overhead of beam training, we propose to train a smaller number of candidate beams and calibrate the beam direction according to the received signals, where how to find proper trained beams that achieve higher accuracy under the fixed training numbers is a

crucial problem. Intuitively, a straightforward scheme is to uniformly sample partial beams [21], [22], whereas its performance could degrade significantly due to the low signal-to-noise ratios (SNRs) when the AoD of the LOS path ϕ_{LOS} does not locate in the main lobe of any sampled beam. Differently, motivated by the two-level beam search where the widebeam codebook can cover the whole angular space with smaller training overhead, we propose to measure the received signals of wide beams for calibrating the beam direction.

Specifically, the calibrated beam training scheme based on the wide beam codebook is proposed. For convenience, we define the received signals of the m -th candidate wide beam as $y_{w,m}$ and concatenate the received signals of all wide beams as the received signal vector $\mathbf{y}_w = [y_{w,1}, y_{w,2}, \dots, y_{w,N_{\text{TX}}/s_{\text{TX}}}]$. Since the narrow beam codebook enjoys higher angular resolution, the calibrated beam training scheme targets to predict the index of the optimal narrow beam at BS side m_0 based on the received signal vector of wide beams \mathbf{y}_w . Because the number of candidate narrow beams is limited, the prediction could be formulated as a multi-classification task, where each classified category corresponds to one candidate narrow beam. Therefore, the prediction model can be represented by the classification function $f_1(\cdot)$ as

$$m_0 = f_1(\mathbf{y}_w), m_0 \in \{1, 2, \dots, N_{\text{TX}}\}. \quad (21)$$

However, the prediction is difficult to be implemented by conventional estimation methods for two reasons. First, the relations between \mathbf{y}_w and ϕ_{LOS} are highly nonlinear, which makes the estimation too complicated. Second, the distribution of the equivalent noise \mathbf{n}_{eq} is difficult to acquire since NLOS paths vary with the propagation environment. Consequently, deep learning which enjoys strong abilities to learn complex nonlinear relations adaptively is introduced to implement the prediction [36]. Besides, we propose to perform the prediction at BS side, whose strong computational capability can ensure low prediction delay.

The deployment of the proposed scheme consists of two stages, i.e., the training stage and the predicting stage. In the training stage, training data is collected to train the deep learning model, where each sample comprises a received signal vector as the model input and the index of the corresponding optimal narrow beam as the classification label, which can be obtained by conventional beam training schemes. After the deep learning model is well-trained by sufficient data, the proposed scheme goes into the predicting stage, where BS and UE only perform the wide beam search, then corresponding received signals are leveraged to predict the optimal

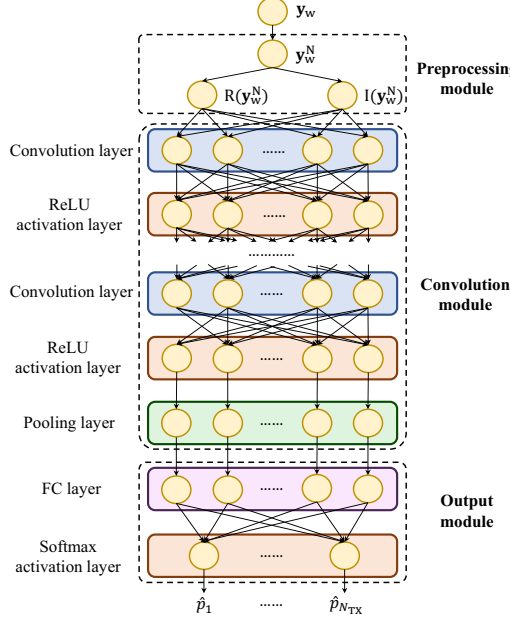


Fig. 2. Proposed CNN based model, where each circle denotes one feature channel.

narrow beam by the well-trained deep learning model, such that the narrow beam search is avoided and the overhead of beam training can be reduced efficiently.

It should be pointed out that the proposed scheme can be extended to more application scenarios. First, the scheme can be utilized to predict the optimal receiving narrow beam at the UE with multiple antennas, since $\mathbf{w}^H \mathbf{a}_{\text{RX}}(\theta_{\text{LOS}})$ can be analysed in a similar manner to Eq. (20). Besides, the scheme can also be adopted in the multi-user scenario, where the calibration of beam directions is performed for each UE separately. Moreover, our proposed scheme can still work well in the NLOS scenario with one dominant cluster, e.g., the reconfigurable intelligent surface (RIS)-assisted scenario [37], [38], where the beam direction is aligned with the AoD of this cluster while other clusters are treated as the noise.

C. Model Design

In this subsection, CNN is adopted to implement the prediction due to its outstanding performance in classification tasks [39]. The proposed CNN based model is depicted in Fig. 2, which can be divided into three parts including the preprocessing module, the convolution module and the output module. For clarification, the following variables with hat denote the predicted results.

Preprocessing module: Since the received signal vector \mathbf{y}_w is complex-valued with large dynamic ranges, which cannot be fed to CNN directly, the preprocessing module firstly normalizes

\mathbf{y}_w by the maximum amplitude of its elements, which can be written as

$$\mathbf{y}_w^N = \frac{\mathbf{y}_w}{\|\mathbf{y}_w\|_\infty}, \quad (22)$$

where \mathbf{y}_w^N denotes the normalized received signal vector. Next, \mathbf{y}_w^N is divided into two real-valued feature channels including its real part $R(\mathbf{y}_w^N)$ and imaginary part $I(\mathbf{y}_w^N)$, which are fed to the following convolution module.

Convolution module: Multiple convolution layers are adopted to extract hidden features from \mathbf{y}_w^N , where each layer is followed by the ReLU activation layer to provide nonlinear fitting ability. Besides, in order to avoid the overwhelmingly complex model, the pooling layer is introduced after the final ReLU activation layer, where each feature channel is downsampled to be a scalar.

Output module: To predict the optimal narrow beam from all candidate narrow beams, the fully-connected (FC) layer is introduced after the pooling layer to implement the size transformation from the extracted features to candidate narrow beams, followed by a softmax activation layer for normalizing the output into probabilities, which can be written as

$$\hat{p}_m = \text{softmax}(\mathbf{w}_m^T \mathbf{v} + b_m), m \in \{1, 2, \dots, N_{\text{TX}}\}, \quad (23)$$

where \hat{p}_m is the predicted probability that the m -th candidate narrow beam is the optimal one, and \mathbf{v} is the output vector of the pooling layer. Additionally, \mathbf{w}_m and b_m denote the weights and bias of the FC layer corresponding to the m -th output. Finally, the narrow beam with the maximum predicted probability is selected, i.e.

$$\hat{m}_0 = \arg \max_{m \in \{1, 2, \dots, N_{\text{TX}}\}} \hat{p}_m. \quad (24)$$

Note that the predicted probabilities provide a judgement of beam qualities, i.e., the beam with larger probability is predicted to enjoy higher beamforming gain compared with the counterpart with smaller probability. Therefore, the additional narrow beam training according to the predicted probabilities can be performed to further calibrate beam directions. Specifically, K_n narrow beams with the top predicted probabilities are trained, where the corresponding indices \mathcal{L}_n can be expressed as

$$\{\hat{p}_{\sigma_1}, \hat{p}_{\sigma_2}, \dots, \hat{p}_{\sigma_{N_{\text{TX}}}}\} = \langle \{\hat{p}_1, \hat{p}_2, \dots, \hat{p}_{N_{\text{TX}}}\} \rangle, \quad (25)$$

$$\mathcal{L}_n = \{\sigma_{N_{\text{TX}}-K_n+1}, \sigma_{N_{\text{TX}}-K_n+1}, \dots, \sigma_{N_{\text{TX}}}\}, \quad (26)$$

and the narrow beam with the maximum power of the received signal is chosen as the optimal one, i.e.

$$\hat{m}_0 = \arg \max_{m \in \mathcal{L}_n} |y_m|^2, \quad (27)$$

where y_m denotes the received signal corresponding to the m -th candidate narrow beam. Obviously, the increase of K_n can improve the beamforming gain but lead to huger training overhead.

Cross entropy loss is one of the evaluation metrics widely used in classification tasks, which is utilized to train our proposed model. Mathematically, it can be expressed as

$$\text{loss} = - \sum_{m=1}^{N_{\text{TX}}} p_m \log \hat{p}_m, \quad (28)$$

where $p_m = 1$ if the m -th candidate narrow beam is the actual optimal one while others equal 0.

IV. LSTM ASSISTED CALIBRATED BEAM TRAINING

A. Motivation

Although the proposed scheme in Section III can reduce the overhead of beam training, the prediction depends on the received signals of only one wide beam training, which lacks robustness to noise. To handle the problem, benefit from the stability of UE movements within a short time, we can utilize prior information to track the UE movement and calculate the AoD of the LOS path ϕ_{LOS} based on the estimated UE location, such that the beam misalignment caused by noise could be calibrated. Beam training is periodically performed in mmWave communication systems, where typical training periods are smaller than 160ms [40]. Besides, because the received signals of beam training are the results of the interaction between the transmitted signals and the propagation environment around BS and UE, these signals draw an RF signature of the UE location [16], [41]. Consequently, prior received signals of beam training could be leveraged to track the UE movement and calibrate the beam direction without additional overhead.

B. Problem Formulation

In this section, the calibrated beam training scheme based on prior received signals of beam training is proposed. Assuming beam training is performed periodically, the received signals of the t -th wide beam training can be represented as $\mathbf{y}_{w,t}$. To predict the optimal narrow beam corresponding to the t -th wide beam training $m_{0,t}$, the received signals of both prior wide beam

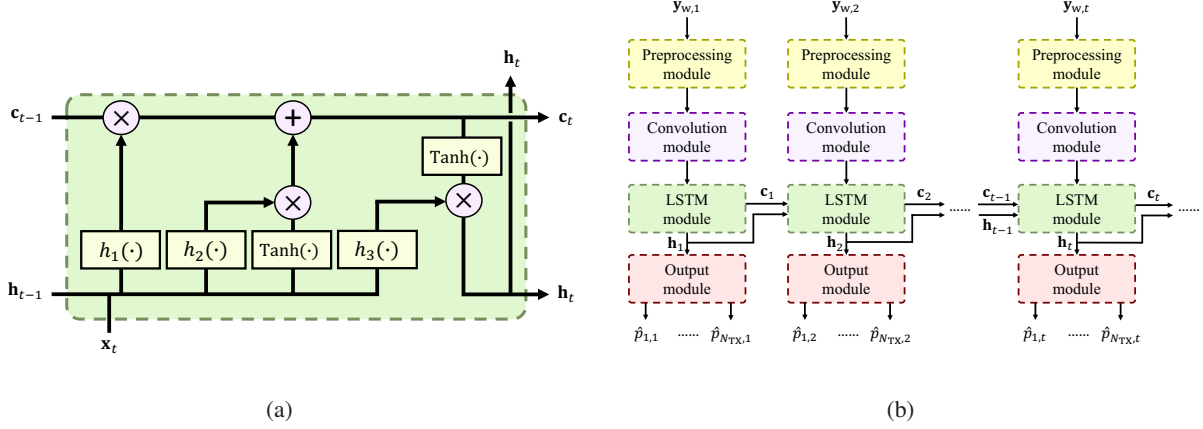


Fig. 3. (a) Basic structure of LSTM, where $h_1(\cdot), h_2(\cdot)$ and $h_3(\cdot)$ denote hidden layers. (b) Proposed LSTM based model.

training $\{y_{w,1}, y_{w,2}, \dots, y_{w,t-1}\}$ and current wide beam training $y_{w,t}$ are jointly utilized, which can be written as

$$m_{0,t} = f_2(y_{w,1}, y_{w,2}, \dots, y_{w,t}), m_{0,t} \in \{1, 2, \dots, N_{TX}\}. \quad (29)$$

Similarly, the prediction is formulated as a multi-classification task, where $f_2(\cdot)$ denotes the classification function. Considering the AoD of the LOS path ϕ_{LOS} varies with the UE movement nonlinearly, we still adopt deep learning models to implement the prediction.

Different from the model deployment in Section III, in order to extract UE movement features, the received signals of wide beam training and corresponding optimal narrow beam indices are packed in time order for each UE, which forms a training sample.

C. Model Design

Specifically, LSTM is used as the prediction model due to its outstanding performance in sequence feature extractions [42]. The basic structure of LSTM is shown in Fig. 3(a), where the input of the current time slot x_t together with the cell state and output of the former time slot $\{c_{t-1}, h_{t-1}\}$ are jointly fed to the LSTM at the t -th time slot, so that LSTM could learn the features from prior inputs.

The proposed LSTM based model is depicted in Fig. 3(b), which reuses partial structures of the CNN based model in Section III. Once the t -th wide beam training is performed, corresponding received signals are firstly fed to the preprocessing and convolution modules to extract preliminary features. Next, the LSTM module further calibrates the narrow beam direction based on the received signals of prior beam training. Finally, the output module

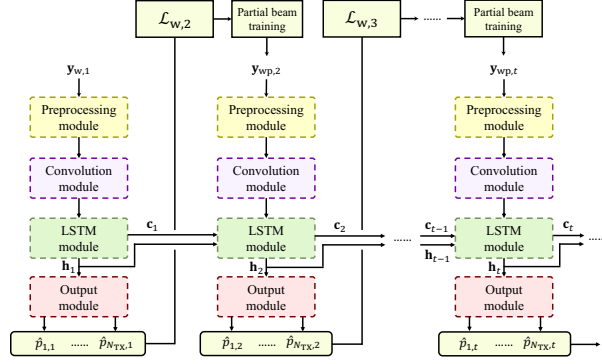


Fig. 4. Proposed adaptive calibrated beam training model.

provides corresponding predicted probabilities $\{\hat{p}_{1,t}, \hat{p}_{2,t}, \dots, \hat{p}_{N_{TX},t}\}$, where the narrow beam with the maximum probability is selected as the predicted optimal beam $\hat{m}_{0,t}$.

Cross entropy loss is still utilized to train the model, where the loss of one training sample is calculated as the average loss of all narrow beam predictions for the UE.

V. ADAPTIVE CALIBRATED BEAM TRAINING

A. Motivation

The proposed schemes in Section III and IV share one disadvantage that wide beam training still brings considerable overhead. However, as shown in Fig. 1, the leaked power of the beams far from the AoD of the LOS path ϕ_{LOS} is small, where effective information is difficult to extract from corresponding received signals due to low SNRs. Therefore, we can train partial wide beams with high SNRs and use corresponding received signals to predict the optimal narrow beam, such that the training overhead can be further reduced in sacrifice of slight beamforming gain. To find the high-SNR wide beams, the stability of UE movements inspires us again that ϕ_{LOS} can be estimated from the received signals of prior beam training. Consequently, we can select the wide beams to be trained based on the prior received signals adaptively.

B. Basic Scheme

Accordingly, we propose the adaptive calibrated beam training scheme, where partial wide beams are selected to be trained based on the received signals of prior beam training. To determine the initial AoD of the LOS path ϕ_{LOS} from the whole angular space, one full wide beam training is performed firstly, where the received signals of all candidate wide beams are measured.

Afterwards, only partial wide beams need training, where the corresponding received signals are utilized to predict the optimal narrow beam index.

For the sake of convenient analysis, the following focuses on the beam selection for the t -th wide beam training, where $t > 1$ and the corresponding AoD of the LOS path is represented as $\phi_{\text{LOS},t}$. Specifically, we define K as the number of the wide beams to be trained, where the corresponding indices are denoted as $\mathcal{L}_{w,t}$. Two criteria are proposed to select the wide beams with high SNRs, which are named optimal neighboring criterion (ONC) and maximum probability criterion (MPC), respectively.

ONC: As indicated in Fig. 1, the wide beam adjacent to the LOS path is more likely to enjoy larger received power, thus ONC targets to select the wide beams whose directions are nearest to $\phi_{\text{LOS},t}$. Unfortunately, $\phi_{\text{LOS},t}$ cannot be accurately known. To find a proper approximation of $\phi_{\text{LOS},t}$, it is noticed that the UE location at the t -th wide beam training is around the location corresponding to the $(t-1)$ -th wide beam training, consequently we propose to use the direction of the previous predicted optimal narrow beam $\gamma_{\text{TX},\hat{m}_{0,t-1}}$ to approximate $\phi_{\text{LOS},t}$. The ONC based beam selection can be mathematically formulated as

$$\gamma_{m,t}^{\Delta} = \text{mod}(|\gamma_{\text{TX},m}^{\text{w}} - \gamma_{\text{TX},\hat{m}_{0,t-1}}|, \pi), m \in \{1, 2, \dots, \frac{N_{\text{TX}}}{s_{\text{TX}}}\}, \quad (30)$$

$$\{\gamma_{\sigma_1,t}^{\Delta}, \gamma_{\sigma_2,t}^{\Delta}, \dots, \gamma_{\sigma_{\frac{N_{\text{TX}}}{s_{\text{TX}}},t}}^{\Delta}\} = \langle \{\gamma_{1,t}^{\Delta}, \gamma_{2,t}^{\Delta}, \dots, \gamma_{\frac{N_{\text{TX}}}{s_{\text{TX}}},t}^{\Delta}\} \rangle, \quad (31)$$

$$\mathcal{L}_{w,t} = \{\sigma_1, \sigma_2, \dots, \sigma_K\}, \quad (32)$$

where the direction difference $|\gamma_{\text{TX},m}^{\text{w}} - \gamma_{\text{TX},\hat{m}_{0,t-1}}|$ modulo π since $|q(\phi_{\text{LOS}})|$ takes π as the period.

MPC: Different from ONC, MPC is based on the property that the predicted probabilities reflect beam qualities. Therefore, MPC selects the wide beams with the top predicted probabilities in the $(t-1)$ -th beam prediction. Nevertheless, the prediction results only provide the probabilities of narrow beams instead of wide beams. To obtain the approximation of the predicted probability for the m -th wide beam $\hat{p}_{m,t}^{\text{w}_{\text{ap}}}$, the predicted probabilities of all narrow beams within the m -th wide beam are added together. Therefore, the MPC based beam selection can be mathematically

formulated as

$$\hat{p}_{m,t}^{\text{Wap}} = \sum_{s=1}^{s_{\text{TX}}} \hat{p}_{(m-1)s_{\text{TX}}+s, t-1}, m \in \{1, 2, \dots, \frac{N_{\text{TX}}}{s_{\text{TX}}}\}, \quad (33)$$

$$\{\hat{p}_{\sigma_1,t}^{\text{Wap}}, \hat{p}_{\sigma_2,t}^{\text{Wap}}, \dots, \hat{p}_{\sigma_{\frac{N_{\text{TX}}}{s_{\text{TX}}}},t}^{\text{Wap}}\} = \langle \{\hat{p}_{1,t}^{\text{Wap}}, \hat{p}_{2,t}^{\text{Wap}}, \dots, \hat{p}_{\frac{N_{\text{TX}}}{s_{\text{TX}}},t}^{\text{Wap}}\} \rangle, \quad (34)$$

$$\mathcal{L}_{\text{w},t} = \{\sigma_{\frac{N_{\text{TX}}}{s_{\text{TX}}}-K+1}, \sigma_{\frac{N_{\text{TX}}}{s_{\text{TX}}}-K+2}, \dots, \sigma_{\frac{N_{\text{TX}}}{s_{\text{TX}}}}\}. \quad (35)$$

Once the t -th partial wide beam training is performed, the corresponding received signal vector $\mathbf{y}_{\text{wp},t}$ can be obtained, given by

$$\mathbf{y}_{\text{wp},t}[m] = \begin{cases} y_{m,t}^{\text{w}}, & \text{if } m \in \mathcal{L}_{\text{w},t}, \\ 0, & \text{else,} \end{cases} \quad (36)$$

where $y_{m,t}^{\text{w}}$ denotes the received signal of the m -th candidate wide beam at the t -th wide beam training. It is noted that the format of $\mathbf{y}_{\text{wp},t}$ is similar to the received signal vector of full wide beam training $\mathbf{y}_{\text{w},t}$, such that the received signal vectors of both full and partial wide beam training can be processed by the same model. Therefore, the prediction model represented by the classification function $f_3(\cdot)$ can be formulated as

$$m_{0,t} = f_3(\mathbf{y}_{\text{w},1}, \mathbf{y}_{\text{wp},2}, \dots, \mathbf{y}_{\text{wp},t}), m_{0,t} \in \{1, 2, \dots, N_{\text{TX}}\}. \quad (37)$$

The proposed adaptive calibrated beam training model is illustrated in Fig. 4. The prediction model structures and loss function are the same as the counterparts in Section IV, whereas the model deployment makes difference. In the training stage, in order to learn to predict the optimal narrow beam from the partial received signals, the model simulates partial wide beam training, i.e., only the received signals of the selected wide beams are used as the model input. In the predicting stage, the proposed scheme only trains the selected wide beams and uses corresponding received signals to predict the optimal narrow beam, so that the overhead of wide beam training can be significantly reduced.

C. Enhanced Adaptive Calibrated Beam Training with Auxiliary LSTM

However, the proposed scheme in Section V-B suffers inherent errors because it selects the wide beams to be trained according to the results in the previous beam prediction, where the prediction will be outdated if the AoD of the LOS path ϕ_{LOS} varies in mobile scenarios. To decrease the errors, considering UE velocities maintain stable in a short time, we can utilize the

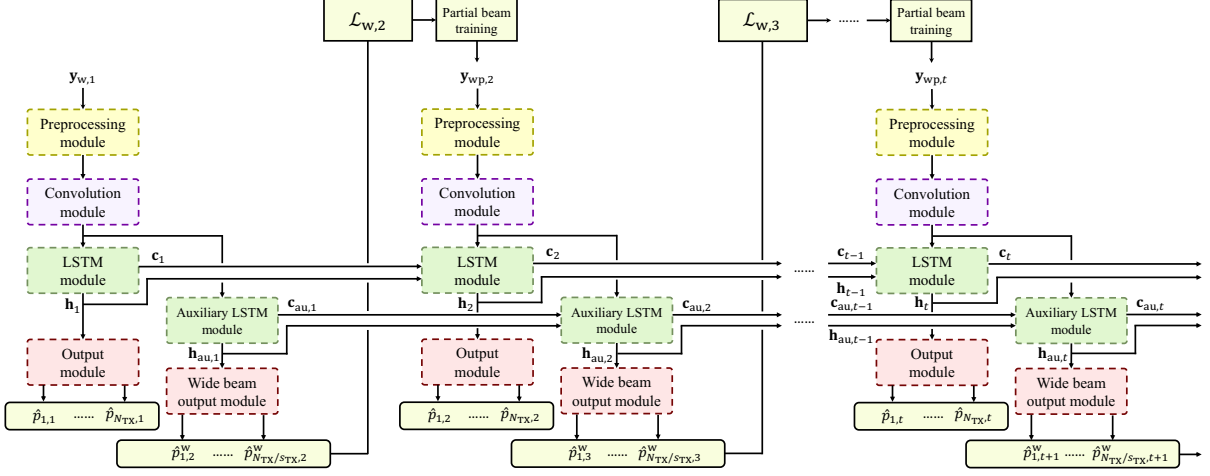


Fig. 5. Proposed adaptive calibrated beam training model, where $c_{au,t}$ and $h_{au,t}$ denote the cell state and output of the auxiliary LSTM, respectively.

received signals of prior beam training to estimate current UE location in advance, such that the indices of the selected wide beams to be trained can be calibrated to further enhance received SNRs.

Specifically, we propose the enhanced adaptive calibrated beam training scheme. To find the wide beams with high SNRs corresponding to the t -th wide beam training, auxiliary LSTM is introduced to predict the t -th optimal wide beam index $m_{0,t}^w$ in advance based on the received signals of prior wide beam training $\{y_w,1, y_w,2, \dots, y_w,t\}$, which can be expressed as

$$m_{0,t}^w = f_{au}(y_w,1, y_w,2, \dots, y_w,t), m_{0,t}^w \in \{1, 2, \dots, \frac{N_{TX}}{s_{TX}}\}, \quad (38)$$

where $f_{au}(\cdot)$ denotes the classification function for the wide beam prediction. Similarly, the output is expressed as the predicted wide beam probabilities $\{\hat{p}_{1,t}^w, \hat{p}_{2,t}^w, \dots, \hat{p}_{N_{TX}/s_{TX},t}^w\}$, where the wide beam with the maximum predicted probability is selected as the optimal wide beam $\hat{m}_{0,t}^w$. Based on the predicted probabilities, ONC selects the wide beams whose directions are nearest to the predicted optimal wide beam, thus Eq. (30) is rewritten as

$$\gamma_{m,t}^\Delta = \text{mod}(|\gamma_{TX,m}^w - \gamma_{TX,\hat{m}_{0,t}^w}^w|, \pi), m \in \{1, 2, \dots, \frac{N_{TX}}{s_{TX}}\}. \quad (39)$$

Besides, MPC selects the wide beams with the top predicted probabilities, where Eq. (34) is rewritten as

$$\{\hat{p}_{\sigma_1,t}^w, \hat{p}_{\sigma_2,t}^w, \dots, \hat{p}_{\sigma_{\frac{N_{TX}}{s_{TX}}},t}^w\} = \langle \{\hat{p}_{1,t}^w, \hat{p}_{2,t}^w, \dots, \hat{p}_{\frac{N_{TX}}{s_{TX}},t}^w\} \rangle. \quad (40)$$

The enhanced adaptive calibrated beam training model is depicted in Fig. 5, where the LSTM module and the proposed auxiliary LSTM module share the same preprocessing and convolution modules to reduce the model overhead, and the wide beam output module is used to obtain the predicted probabilities of the wide beam prediction. For the model deployment, auxiliary LSTM does not require to collect extra training data in the training stage. Once the t -th wide beam training is performed, the wide beam index with the maximum power of the received signal is used as the classification label of the wide beam prediction.

Similarly, cross entropy loss is used as the loss function in wide beam predictions. To train the whole model with auxiliary LSTM, the losses of both narrow beam predictions loss_n and wide beam predictions loss_w are summed up with the weight coefficient μ , which can be expressed as

$$\text{loss} = \text{loss}_n + \mu \text{loss}_w, \quad (41)$$

VI. SIMULATION ANALYSIS

A. Simulation Setup

We consider a mmWave wireless communication system serving one single-antenna UE, where the LOS scenario is assumed. To verify the reliability of our proposed schemes, we assume the mobile scenario where UE performs the uniformly variable rectilinear motion with speed $v_{\text{UE}} \in [10, 50]\text{m/s}$ and acceleration $a_{\text{UE}} \in [-8, 8]\text{m/s}^2$, and the direction is randomly generated in $[0, 2\pi]$. In order to simulate the channel variations with UE movements, we apply the COST 2100 channel model [43], [44], which defines several groups of far scatterers in the space and each group corresponds to one NLOS cluster together with a visible region, i.e., the area where the cluster exists. Based on the locations of BS, UE and far scatterers, the channel matrix \mathbf{H} could be generated by Eq. (1). Specific parameters of the mmWave communication system are shown in Table. I. The power of AWGN σ^2 is calculated as $(-174 + 10 \log_{10} W + N_F)\text{dBm}$, where the noise factor $N_F = 6\text{dB}$. Moreover, the pathloss PL is obtained as $\text{PL} = (26 \log_{10} d + 20 \log_{10} f_c - 147.56)\text{dB}$ [44], where d denotes the propagation distance.

For the proposed deep learning models, the detailed structures and parameters are shown in Table. II, where f_i and f_o denote the numbers of input feature channels and output feature channels. Besides, the parameters in convolution layers (p_1, p_2, p_3) represent the kernel size, sampling stride and zero-padding size, respectively. To accelerate model convergence, batch normalization (BN) is applied in the convolution module, which transforms the processed data

TABLE I
SYSTEM PARAMETERS.

Parameter	Value
Center frequency f_c	28GHz
Bandwidth W	2MHz
Group number of far scatterers n_g	15
Path number within one cluster L_c	20
Visible region radius r_v	40m
AoD spread within one cluster $\Delta\phi_c$	2.4°
Delay spread within one cluster $\Delta\tau_c$	5ns
Shadow fading standard deviation σ_{SF}	4dB
Ricean K factor K_R	8dB
BS antenna number M_{TX}	64
BS wide beam number N_{TX}/s_{TX}	16
BS narrow beam number N_{TX}	64
Beam training period τ	100ms
Total beam training number T	10
Cell radius r	100m
Transmit power P	15dBm

TABLE II
STRUCTURES AND PARAMETERS OF PROPOSED DEEP LEARNING MODELS.

Module	Layer	Parameter
Convolution module	Convolution	$f_i = 2, f_o = 64, (3, 3, 1)$, BN
	ReLU activation	$f_i = 64, f_o = 64$
	Convolution	$f_i = 64, f_o = 256, (3, 1, 1)$, BN
	ReLU activation	$f_i = 256, f_o = 256$
LSTM module	Pooling	$f_i = 256, f_o = 256$, max-pooling
	LSTM	$f_i = 256, f_o = 256$, dropout = 0.2
	LSTM	$f_i = 256, f_o = 256$, dropout = 0.2
	Auxiliary	$f_i = 256, f_o = 256$, dropout = 0.2
LSTM module	LSTM	$f_i = 256, f_o = 256$, dropout = 0.2
	Output	FC
	module	$f_i = 256, f_o = 64$, dropout = 0.3
	Softmax activation	$f_i = 64, f_o = 64$
Wide beam output module	FC	$f_i = 256, f_o = 16$, dropout = 0.3
	Softmax activation	$f_i = 16, f_o = 16$

to the standard distribution with mean 0 and variance 1 [45]. Furthermore, LSTM layers and FC layers exploit dropout strategy to abandon part of neurons randomly in the training stage for preventing overfitting [46].

We construct a dataset with 20,480 samples, where 80% and 20% of the dataset is used as the training set and the validation set, respectively. The model is trained for 80 epochs in the training stage, where Adam optimizer based on the back propagation algorithm is used to optimize model parameters [47]. Furthermore, the weight coefficient in the enhanced calibrated beam training scheme μ is set to be 1.

Normalized beamforming gain G_N is utilized for performance evaluations. For one prediction, G_N can be calculated as

$$G_N = \frac{|\mathbf{H}\mathbf{f}_{\hat{m}_0}|^2}{|\mathbf{H}\mathbf{f}_{m_0}|^2}, \quad (42)$$

where \mathbf{f}_{m_0} and $\mathbf{f}_{\hat{m}_0}$ denote the actual optimal narrow beam and the predicted optimal narrow beam, respectively. The ultimate G_N is the average results of the whole validation set in 5 times of model training.

The source code of our simulations can be referred in [48]. For simplicity, calibrated beam training is written as CBT in the following figures.

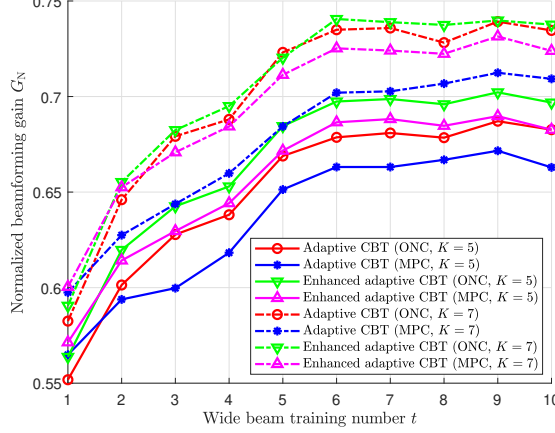


Fig. 6. Normalized beamforming gain comparison under different wide beam training numbers.

B. Scheme Analysis

In this subsection, we present the simulation results to analyze the proposed adaptive calibrate beam training scheme.

Firstly, we investigate the impact of the number of wide beam training t on the normalized beamforming gain G_N , where the results under the number of trained wide beams $K = 5, 7$ are shown in Fig. 6. It can be seen that G_N increases with t for both ONC and MPC based schemes, which is because more prior received signals can provide more accurate UE movement information. After $t = 6$, G_N converges in all simulation scenarios. Besides, the increase of G_N also demonstrates that both ONC and MPC can select the wide beams with high SNRs effectively. Moreover, the performance of the enhanced adaptive scheme is better than its basic counterpart, which validates that auxiliary LSTM can reduce the errors of tracking UE locations in mobile scenarios.

Next, Fig. 7 shows the impact of the number of trained wide beams K on the normalized beamforming gain G_N , where the results are the average when $t \geq 6$. Considering the symmetry of neighboring wide beams, the ONC based enhanced adaptive scheme only shows the results under odd K . We can see that G_N increases with K since the deep learning model can extract more robust features from the received signals of more wide beams. Besides, it further validates that G_N of the enhanced adaptive scheme surpasses its basic counterpart. Moreover, it is observed that the performance of ONC is better than MPC especially when K is small. This is because noise and multipath interference may lead MPC to select irregular indices of wide beams, which could bring difficulties for the deep learning model to extract stable features. One example under

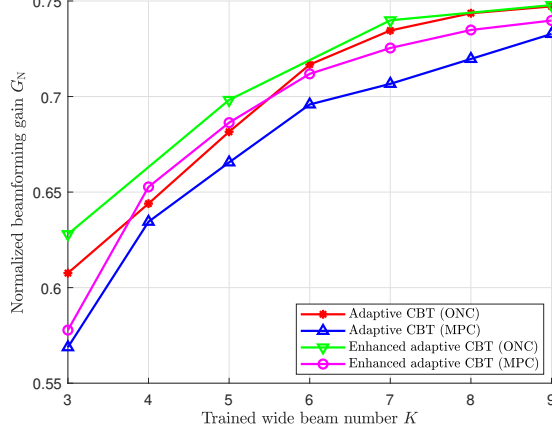


Fig. 7. Normalized beamforming gain comparison under different trained wide beam numbers.

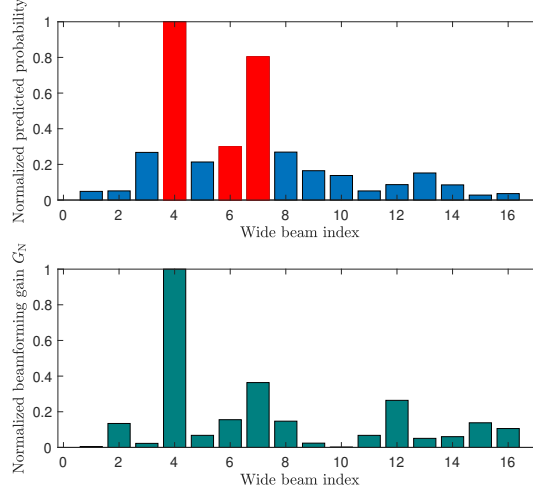


Fig. 8. Comparison between normalized predicted probabilities and normalized beamforming gains of wide beams under the MPC based enhanced adaptive calibrated beam training scheme, where red columns denote the selected wide beams to be trained.

$K = 3$ is illustrated in Fig. 8, where the predicted probabilities have several local maximums due to the noise and NLOS paths. More seriously, this may make MPC ignore the neighboring wide beams of the strongest wide beam especially under small K , which could lead the prediction model to fail to track the beam switch in mobile scenarios. Accordingly, we adopt the ONC based enhanced adaptive scheme in the following simulations.

C. Performance Comparison

In this subsection, we compare the performance of our proposed schemes with two baselines. Baseline 1 proposed to calculate the optimal narrow beam direction based on the ratio of the beamforming gains between the selected wide beam and its neighboring wide beams [13], while

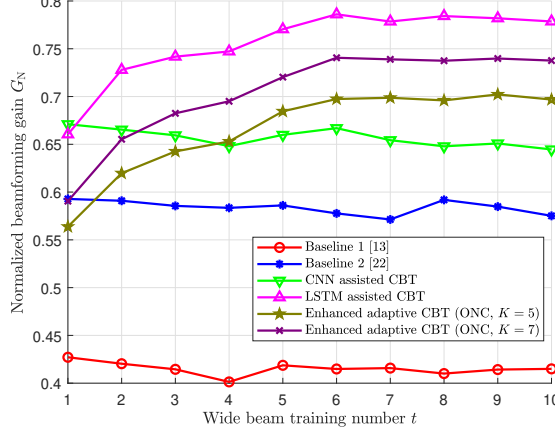


Fig. 9. Normalized beamforming gain comparison under different wide beam training numbers.

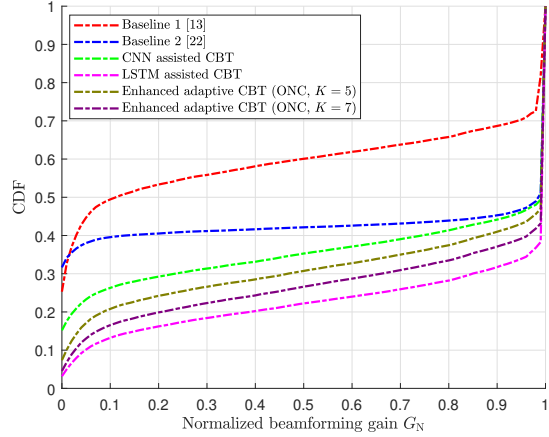


Fig. 10. Normalized beamforming gain CDF comparison.

baseline 2 is the deep learning based beam prediction scheme by using the training results of uniformly sampled beams [22]. For proper comparison, the prediction in [22] is implemented by the same deep learning model as our proposed schemes, and the beam sampling interval is set to be 4 for guaranteeing equal training overhead.

Firstly, we investigate the impact of the number of wide beam training t on the normalized beamforming gain G_N in Fig. 9, where both baselines and the CNN assisted scheme do not rely on the prior information and thus maintain stable G_N . Obviously, the performance of our proposed schemes all surpasses the baselines. Similar to Fig. 6, G_N increases with t in the LSTM assisted scheme and the enhanced adaptive scheme. Furthermore, although both of the LSTM assisted and enhanced adaptive schemes adopt the same input in the initial full wide beam training, the performance of the latter scheme decreases as K . This is because the input

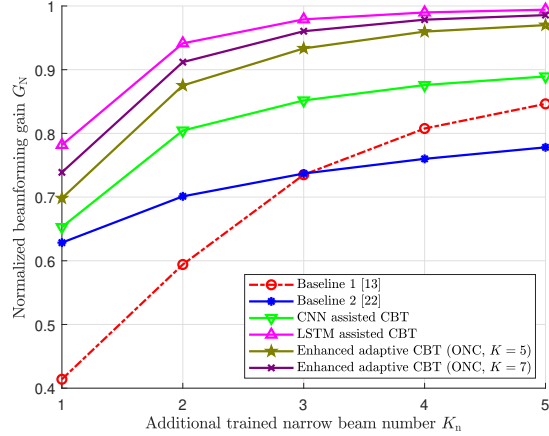


Fig. 11. Normalized beamforming gain comparison under different additional trained narrow beam numbers.

format difference between full beam training and partial beam training could become larger under smaller K , which makes the prediction model harder to extract compatible features from both kinds of inputs.

To show the superiority of our proposed schemes, we compare the cumulative distribution function (CDF) of the normalized beamforming gain G_N in Fig. 10. Note that the following results focus on the average G_N when the model has converged, i.e., $t \geq 6$. First, we investigate the impact of input formats by comparing the CNN assisted scheme with baselines. Compared with baseline 1, the CNN assisted scheme can enhance the accuracy of beam predictions since our scheme can extract more robust features from the received signals of all wide beams. Compared with baseline 2, the CNN assisted scheme can estimate the rough range of the optimal narrow beam more accurately and still obtain the suboptimal narrow beam when the beam direction is not perfectly aligned. This is because wide beams can achieve greater angular coverage than the sampled narrow beams used in baseline 2. Next, the comparison between the CNN assisted scheme and the LSTM assisted scheme demonstrates that prior information can decrease wrong predictions efficiently. Besides, it can be seen that the enhanced adaptive scheme can significantly reduce training overhead in sacrifice of slight prediction accuracy.

In our proposed schemes, the additional narrow beam training can be performed to further calibrate beam directions according to the predicted probabilities. Here, we investigate the impact of the number of trained narrow beams K_n on the normalized beamforming gain G_N in Fig. 11. It can be observed that the additional narrow beam training can improve G_N for all schemes. Besides, our proposed schemes achieve more remarkable performance enhancement than baseline

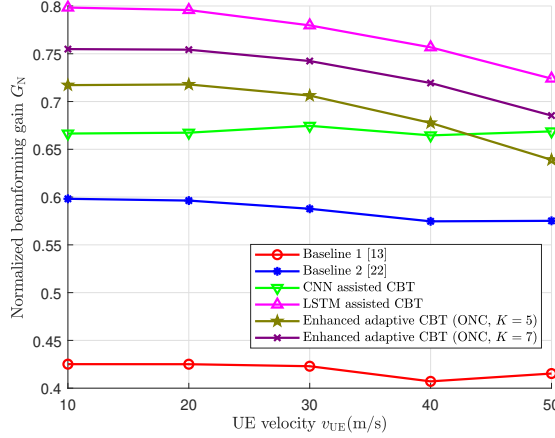


Fig. 12. Normalized beamforming gain comparison under different UE velocities.

2 when K_n becomes larger, which validates again that our schemes can estimate the rough range of the optimal narrow beam more accurately. Moreover, it is delightful to see that the enhanced adaptive scheme with $K = 5, K_n = 4$ achieves almost perfect beam alignment $G_N = 96.0\%$, which indicates that our proposed scheme could significantly reduce the overhead of beam training as well as maintain high beamforming gain.

Next, the impact of UE velocities v_{UE} on the normalized beamforming gain G_N is illustrated in Fig. 12. Similar to Fig. 9, the performance of baselines and the proposed CNN assisted scheme maintains stable since they do not rely on the prior information. For our proposed LSTM assisted scheme and enhanced adaptive scheme, G_N keeps stable when v_{UE} is below 20m/s, which indicates that LSTM can track UE movements well. As v_{UE} further increases, the prediction performance degrades gradually, because the serious nonlinearity caused by UE movements makes the tracking more difficult.

Finally, we investigate the impact of the transmit power P on the normalized beamforming gain G_N in Fig. 13. Obviously, G_N increases with P owing to higher SNRs. Besides, the CNN assisted scheme achieves larger performance enhancement than baseline 2 as P increases, which further verifies the advantage of our proposed scheme in high SNR scenarios that wide beams can implement greater angular coverage than the sampled narrow beams.

VII. CONCLUSIONS

In order to reduce the overhead of mmWave beam training, the deep learning assisted calibrated beam training scheme is proposed in this paper. First of all, the feasibility of estimating the

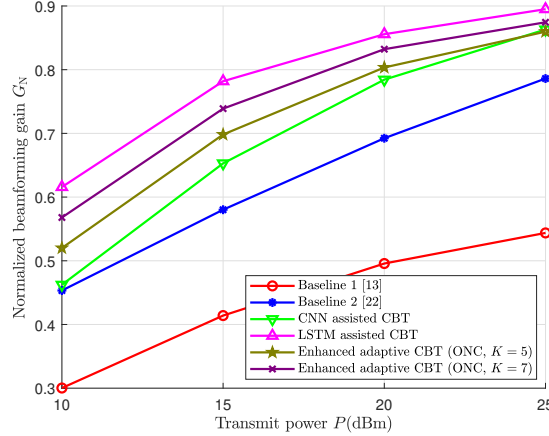


Fig. 13. Normalized beamforming gain comparison under different transmit powers.

angle of the dominant path based on the channel power leakage in the received signals of beam training is elaborated. Accordingly, three schemes are proposed to predict the optimal narrow beam according to the received signals of wide beam training, where deep learning models are utilized to handle the highly nonlinear properties of the channel power leakage. In the first scheme, CNN is adopted to predict the beam based on the instantaneous received signals. Besides, the additional narrow beam training according to the predicted probabilities is proposed to further calibrate beam directions. In the second scheme, LSTM is adopted to track the movement of UEs and calibrate the beam direction based on the received signals of prior beam training. In the third scheme, we propose an adaptive beam training strategy where partial wide beams are selected to be trained based on the prior received signals. Two criteria, namely ONC and MPC, are designed for the selection, where ONC selects the neighboring wide beams of the previous predicted optimal narrow beam, while MPC selects the wide beams with the top predicted probabilities in the previous beam prediction. To handle mobile scenarios, auxiliary LSTM is introduced to calibrate the directions of the selected wide beams more precisely. Simulation results demonstrate that our proposed schemes achieve significantly higher beamforming gain as well as smaller beam training overhead compared with the conventional counterparts.

REFERENCES

- [1] M. Xiao et al., “Millimeter wave communications for future mobile networks,” *IEEE J. Sel. Areas Commun.*, vol. 35, no. 9, pp. 1909–1935, Sep. 2017.
- [2] S. K. Sharma, T. E. Bogale, L. B. Le, S. Chatzinotas, X. Wang, and B. Ottersten, “Dynamic spectrum sharing in 5G wireless networks with full-duplex technology: recent advances and research challenges,” *IEEE Commun. Surv. Tuts.*, vol. 20, no. 1, pp. 674–707, Jan.–Mar. 2018.

- [3] T. S. Rappaport et al., "Millimeter wave mobile communications for 5G cellular: it will work!," *IEEE Access*, vol. 1, pp. 335–349, May 2013.
- [4] Y. Zeng, R. Zhang, and T. J. Lim, "Wireless communications with unmanned aerial vehicles: opportunities and challenges," *IEEE Commun. Mag.*, vol. 54, no. 5, pp. 36–42, May 2016.
- [5] A. Alkhateeb, O. El Ayach, G. Leus, and R. W. Heath, "Channel estimation and hybrid precoding for millimeter wave cellular systems," *IEEE J. Sel. Topics Signal Process.*, vol. 8, no. 5, pp. 831–846, Oct. 2014.
- [6] X. Sun, C. Qi, and G. Y. Li, "Beam training and allocation for multiuser millimeter wave massive MIMO systems," *IEEE Trans. Wireless Commun.*, vol. 18, no. 2, pp. 1041–1053, Feb. 2019.
- [7] Z. Sha, Z. Wang, S. Chen, and L. Hanzo, "Graph theory based beam scheduling for inter-cell interference avoidance in mmWave cellular networks," *IEEE Trans. Veh. Tech.*, vol. 69, no. 4, pp. 3929–3942, Apr. 2020.
- [8] C. Jeong, J. Park, and H. Yu, "Random access in millimeter-wave beamforming cellular networks: issues and approaches," *IEEE Commun. Mag.*, vol. 53, no. 1, pp. 180–185, Jan. 2015.
- [9] T. Baykas, M. A. Rahman, R. Funada, F. Kojima, H. Harada, and S. Kato, "Beam codebook based beamforming protocol for multi-Gbps millimeter-wave WPAN systems," *IEEE J. Sel. Areas Commun.*, vol. 27, no. 8, pp. 1390–1399, Oct. 2009.
- [10] J. Wang, Z. Lan, C. Sum, C. Pyo, J. Gao, T. Baykas, A. Rahman, R. Funada, F. Kojima, I. Lakkis, H. Harada, and S. Kato, "Beamforming codebook design and performance evaluation for 60GHz wideband WPANs," in *Proc. IEEE Veh. Tech. Conf. (VTC)*, Sep. 20–23, 2009, pp. 1–6.
- [11] F. Dai, and J. Wu, "Efficient broadcasting in ad hoc wireless networks using directional antennas," *IEEE Trans. Parallel and Distrib. Syst.*, vol. 17, no. 4, pp. 335–347, Apr. 2006.
- [12] J. Kim, and A. F. Molisch, "Fast millimeter-wave beam training with receive beamforming," *J. Commun. Netw.*, vol. 16, no. 5, pp. 512–522, Oct. 2014.
- [13] X. Luo, W. Liu, and Z. Wang, "Calibrated beam training for millimeter-wave massive MIMO systems," in *Proc. IEEE Veh. Tech. Conf. (VTC)*, Sep. 22–25, 2019, pp. 1–5.
- [14] F. B. Mismar, B. L. Evans, and A. Alkhateeb, "Deep reinforcement learning for 5G networks: joint beamforming, power control, and interference coordination," *IEEE Trans. Commun.*, vol. 68, no. 3, pp. 1581–1592, Mar. 2020.
- [15] W. Ma, C. Qi, Z. Zhang, and J. Cheng, "Sparse channel estimation and hybrid precoding using deep learning for millimeter wave massive MIMO," *IEEE Trans. Commun.*, vol. 68, no. 5, pp. 2838–2849, May 2020.
- [16] A. Alkhateeb, S. Alex, P. Varkey, Y. Li, Q. Qu, and D. Tujkovic, "Deep learning coordinated beamforming for highly-mobile millimeter wave systems," *IEEE Access*, vol. 6, pp. 37328–37348, Jun. 2018.
- [17] K. Ma, P. Zhao, and Z. Wang, "Deep learning assisted beam prediction using out-of-band information," in *Proc. IEEE Veh. Tech. Conf. (VTC)*, May 25–28, 2020, pp. 1–5.
- [18] M. Alrabeiah, and A. Alkhateeb, "Deep learning for mmWave beam and blockage prediction using sub-6 GHz channels," *IEEE Trans. Commun.*, vol. 68, no. 9, pp. 5504–5518, Sep. 2020.
- [19] M. Alrabeiah, A. Hredzak, Z. Liu, and A. Alkhateeb, "ViWi: a deep learning dataset framework for vision-aided wireless communications," in *Proc. IEEE Veh. Tech. Conf. (VTC)*, May 25–28, 2020, pp. 1–5.
- [20] M. Alrabeiah, A. Hredzak, and A. Alkhateeb, "Millimeter wave base stations with cameras: vision-aided beam and blockage prediction," in *Proc. IEEE Veh. Tech. Conf. (VTC)*, May 25–28, 2020, pp. 1–5.
- [21] T. Chang, L. Shen, and K. Feng, "Learning-based beam training algorithms for IEEE802.11ad/ay networks," in *Proc. IEEE Veh. Tech. Conf. (VTC)*, Apr. 28–May 1, 2019, pp. 1–5.
- [22] C. Qi, Y. Wang, and G. Y. Li, "Deep learning for beam training in millimeter wave massive MIMO systems," accepted by *IEEE Trans. Wireless Commun.*, early access, doi: 10.1109/TWC.2020.3024279.

- [23] V. Va, H. Vikalo, and R. W. Heath, "Beam tracking for mobile millimeter wave communication systems," in *Proc. IEEE Global Conf. Signal Inf. Process. (GlobalSIP)*, Dec. 7–9, 2016, pp. 743–747.
- [24] S. Jayaprakasam, X. Ma, J. W. Choi, and S. Kim, "Robust beam-tracking for mmWave mobile communications," *IEEE Commun. Lett.*, vol. 21, no. 12, pp. 2654–2657, Dec. 2017.
- [25] J. Lim, H. Park, and D. Hong, "Beam tracking under highly nonlinear mobile millimeter-wave channel," *IEEE Commun. Lett.*, vol. 23, no. 3, pp. 450–453, Mar. 2019.
- [26] Y. Liu, Z. Jiang, S. Zhang, and S. Xu, "Deep reinforcement learning based beam tracking for low-latency services in vehicular networks," in *Proc. IEEE Int. Commun. Conf. (ICC)*, Jun. 7–11, 2020, pp. 1–7.
- [27] S. Chen, Z. Jiang, S. Zhou, and Z. Niu, "Time-sequence channel inference for beam alignment in vehicular networks," in *Proc. IEEE Global Conf. Signal Inf. Process. (GlobalSIP)*, Nov. 26–29, 2018, pp. 1199–1203.
- [28] T. Xie, L. Dai, D. W. K. Ng, and C. B. Chae, "On the power leakage problem in millimeter-wave massive MIMO with lens antenna arrays," *IEEE Trans. Signal Process.*, vol. 67, no. 18, pp. 4730–4744, Jul. 2019.
- [29] T. Bai, and R. W. Heath, "Coverage and rate analysis for millimeter-wave cellular networks," *IEEE Trans. Wireless Commun.*, vol. 14, no. 2, pp. 1100–1114, Feb. 2015.
- [30] T. S. Rappaport, Y. Xing, G. R. MacCartney, A. F. Molisch, E. Mellios, and J. Zhang, "Overview of millimeter wave communications for fifth-generation (5G) wireless networks—with a focus on propagation models," *IEEE Trans. Antennas Propag.*, vol. 65, no. 12, pp. 6213–6230, Dec. 2017.
- [31] A. A. M. Saleh, and R. Valenzuela, "A statistical model for indoor multipath propagation," *IEEE J. Sel. Areas Commun.*, vol. 5, no. 2, pp. 128–137, Feb. 1987.
- [32] K. Chen, C. Qi, and G. Y. Li, "Two-step codeword design for millimeter wave massive MIMO systems with quantized phase shifters," *IEEE Trans. Signal Process.*, vol. 68, no. 1, pp. 170–180, Jan. 2020.
- [33] Z. Xiao, T. He, P. Xia, and X. G. Xia, "Hierarchical codebook design for beamforming training in millimeter-wave communication," *IEEE Trans. Wireless Commun.*, vol. 15, no. 5, pp. 3380–3392, May 2016.
- [34] W. Roh et al., "Millimeter-wave beamforming as an enabling technology for 5G cellular communications: theoretical feasibility and prototype results," *IEEE Commun. Mag.*, vol. 52, no. 2, pp. 106–113, Feb. 2014.
- [35] A. L. Swindlehurst, E. Ayanoglu, P. Heydari, and F. Capolino, "Millimeterwave massive MIMO: the next wireless revolution?" *IEEE Commun. Mag.*, vol. 52, no. 9, pp. 56–62, Sep. 2014.
- [36] K. Hornik, M. Stinchcombe, and H. White, "Multilayer feedforward networks are universal approximators," *Neural Netw.*, vol. 2, no. 5, pp. 359–366, 1989.
- [37] C. Liaskos, S. Nie, A. Tsoliariadou, A. Pitsillides, S. Ioannidis, and I. Akyildiz, "A new wireless communication paradigm through softwarecontrolled metasurfaces," *IEEE Commun. Mag.*, vol. 56, no. 9, pp. 162–169, Sep. 2018.
- [38] Z. Zhou, N. Ge, Z. Wang, and L. Hanzo, "Joint transmit precoding and reconfigurable intelligent surface phase adjustment: a decomposition-aided channel estimation approach," accepted by *IEEE Trans. Commun.*, early access, doi: 10.1109/TCOMM.2020.3034259.
- [39] A. Krizhevsky, I. Sutskever, and G. E. Hinton, "ImageNet classification with deep convolutional neural networks," in *Proc. Neural Info. Process. Syst. (NIPS)*, Dec. 3–6, 2012, pp. 1–9.
- [40] M. Giordani, M. Polese, A. Roy, D. Castor, and M. Zorzi, "A tutorial on beam management for 3GPP NR at mmWave frequencies," *IEEE Commun. Surv. Tuts.*, vol. 21, no. 1, pp. 173–196, Jan.–Mar. 2019.
- [41] J. Vieira, E. Leitinger, M. Sarajlic, X. Li, and F. Tufvesson, "Deep convolutional neural networks for massive MIMO fingerprint-based positioning," in *Proc. IEEE Annu. Int. Symp. Pers., Indoor, Mobile Radio Commun. (PIMRC)*, Oct. 8–13, 2017, pp. 1–6.

- [42] T. Wang, C. Wen, S. Jin, and G. Y. Li, “Deep learning-based CSI feedback approach for time-varying massive MIMO channels,” *IEEE Wireless Commun. Lett.*, vol. 8, no. 2, pp. 416–419, Apr. 2019.
- [43] L. Liu et al., “The COST 2100 MIMO channel model,” *IEEE Wireless Commun.*, vol. 19, no. 6, pp. 92–99, Dec. 2012.
- [44] *COST 2100 Channel Model*, Implementation Available in the Public Domain. Accessed: Jan. 1, 2021. [Online]. Available: <https://github.com/cost2100>.
- [45] Ioffe, Sergey, and C. Szegedy, “Batch normalization: accelerating deep network training by reducing internal covariate shift,” in *Proc. Int. Conf. Mach. Learn. (ICML)*, Jul. 6–11, 2015, pp. 448–456.
- [46] N. Srivastava, G. Hinton, A. Krizhevsky, I. Sutskever, and R. Salakhutdinov, “Dropout: a simple way to prevent neural networks from overfitting,” *J. Mach. Learn. Res.*, vol. 15, pp. 1929–1958, Jun. 2014.
- [47] D. P. Kingma, and J. L. Ba, “Adam: a method for stochastic optimization”, *arXiv preprint arXiv:1412.6980*, 2014.
- [48] *Deep learning assisted calibrated beam training*, Implementation Available in the Public Domain. Accessed: Jan. 7, 2021. [Online]. Available: <https://github.com/KeMa1998/DL-assisted-calibrated-beam-training>.